



New approach to production of fiber reinforced polymer hybrid composites



Victor Beloshenko^a, Yuri Voznyak^{b,*}, Andrei Voznyak^c, Bogdan Savchenko^d

^a Donets Institute for Physics and Engineering named after A.A. Galkin, National Academy of Sciences of Ukraine, pr. Nauki 46, 03028 Kyiv, Ukraine

^b Centre of Molecular and Macromolecular Studies, Polish Academy of Sciences, Sienkiewicza Street, 112, 90363 Lodz, Poland

^c Donetsk National University of Economics and Trade named M. Tugan-Baranovsky, Kurchatov Street, 13, 50042 Krivoy Rog, Ukraine

^d Kyiv National University of Technologies and Design, Nemirovicha Danchenko Street, 2, 01011 Kyiv, Ukraine

ARTICLE INFO

Article history:

Received 16 July 2016

Received in revised form

23 September 2016

Accepted 16 December 2016

Available online 18 December 2016

Keywords:

Hybrid

Polymer-matrix composites (PMCs)

Microstructures

Plastic deformation

Electron microscopy

Extrusion

ABSTRACT

This study addresses the new approach into production of fiber-based hybrid composites, that is in-situ formation of polymer fiber net out of polymeric matrix combined with simultaneous orientation of the foreign filler fibers. Such hybrid composite can consist of three and more components, including filler fibers, polymer fibers and a non-oriented polymer matrix. This possibility is demonstrated with using the system of linear low-density polyethylene – basalt fibers (LLDPE/BFs). The hybrid effect (double Young's modulus, yield stress higher by the factor of 1.3, triple impact strength of LLDPE) is achieved owing to self-reinforcing process and enhancing of the interfacial interaction as a result of fiber orientation and formation of effective physical entanglements between the BFs and the net of interwoven LLDPE fibers.

© 2016 Elsevier Ltd. All rights reserved.

1. Introduction

Nowadays, high attention is attracted into production of polymeric hybrid composites [1,2]. They are formed by incorporating of two and more reinforcing materials to a polymeric matrix. The reinforcing (foreign) materials provide a synergetic effect called a “hybrid effect” that determines new or enhanced properties (improved Young's modulus, ductility, light weight, flame retarding ability, etc). The hybrid composites based on fiber fillers have become extremely important materials [3,4]. They are widely used in aerospace, automotive, and construction industry etc. The main requirements placed upon the fibers used for fabricating the hybrid composites are their strength, lightweight, durability and competitiveness. The abovementioned requirements are met by a limited number on organic and inorganic fibers [5]. The glass and carbon fibers are well-known fibers used on an industrial scale. The main drawback of composites containing glass or carbon fibers is the brittleness and the expense of production in the case of carbon fibers. Basalt fibers (BFs) can be also considered as a prospective

type of reinforcing material for the fabricating of hybrid composites. The tensile and compressive properties of BFs are better than those of the fibers of E-glass and they are cheaper than the carbon fibers [6]. BFs are characterized by high temperature resistance, excellent stability, good chemical resistance. Besides, they are non-toxic, natural, and eco-friendly [6].

The physical and mechanical properties of the hybrid composites based on fiber fillers can be varied by different methods: incorporation of foreign fillers like nanoparticles [7–12], surface alteration of the fibers [13–16] and hybridization with different fibers [17–23]. The last way provides the widest opportunities for production of different types of hybrid composites. In this case, the properties are determined by both the composition and the relative positions of the reinforcing fibers. In particular, Park and Jang [24] fabricated the hybrid composite material containing polyethylene and carbon fibers within an epoxy matrix. It was shown that if the carbon fibers are located at the periphery, and the ductile polyethylene fibers are placed at the center, the composite demonstrates a high degree of flexural strength. Sarasini et al. [25] reported that the hybrid composite containing alternating fabric layers of basalt and carbon (basalt-carbon-basalt, 3-7-3 layers) possessed better absorption of impact energy than the laminates consisting of only carbon fibers. In a similar way, Zhang et al. [26]

* Corresponding author.

E-mail address: wozniak@cbmm.lodz.pl (Y. Voznyak).

registered a synergistic strength effect in a hybrid composite containing BFs reinforced with polybutylene succinate fibers. Besides, so-called “in-situ hybrid” composites can be produced, i.e. the systems where the polymer matrices are reinforced by both organic and inorganic fibers. Examples are composites containing thermotropic liquid crystalline polymers, which form fibrils during processing [27,28]. At the same time, a reinforcement effect is provided, an abrasive effect of inorganic fibers is reduced, and processability of the composites is improved.

A possible alternative way to enhance the properties of hybrid composites can be fabrication of self-reinforced hybrid composites. In this case, another reinforcing fibers are manufactured from a highly oriented form of the same polymer matrix. An advantage is that the polymer fibers demonstrate an effect of self-reinforcing of the polymeric matrix, with better specific stiffness and specific strength, toughness and ductility provided. Besides, the polymer fibers are directly bound to the polymer matrix. They can facilitate the formation of physical entanglements between the reinforcing filler fibers and the polymer matrix.

The basic methods of self-reinforced polymeric materials production are solid-phase extrusion forming (drawing, rolling, ram and hydrostatic extrusion) and the techniques exploiting melt shearing [29]. At the moment, the equal-channel angular extrusion (ECAE) is an innovative process that affects microstructures through extreme uniform simple shear [30]. Many polymer systems such as low- and high-density polyethylenes, poly(ethylene terephthalate), polycarbonate, polymethylmethacrylate, polyamide-6 have been shear-deformed by ECAE to create self-reinforced polymeric materials [30]. Contrary to rolling, drawing, and ram extrusion, ECAE is the only one process that preserves the sample shape [30]. Besides, ECAE is able to produce more uniform distribution and better dispersion of the filler within the polymeric matrix [31,32]. ECAE can control the fiber orientation as well as a fiber lengths distribution [33–36]. The use of a modified ECAE version (namely, equal-channel multiple-angular extrusion (ECMAE)) allows creation of a controlled biaxial orientation [37]. The last fact is of special importance because formation of a biaxial

fiber stacking is the basis of development of different types of woven fabrics. The woven fabrics are one of the most effective reinforcing structures [6]. So, biaxially oriented fiber fillers and polymeric fibers within the matrix act jointly as load bearing components and can provide an effect analogous to incorporation of different types of the woven fabrics.

In the present work, a new approach to development of BFs-based hybrid composites is considered. The key point is reinforcing of the polymeric matrix by interwoven fibrils that are formed directly out of the polymer matrix during solid-phase extrusion. As an extrusion method, ECMAE was selected in order to provide biaxial orientation of both types of the fibers. This kind of processing is able to form a self-reinforcing structure characterized by enhanced strength, toughness, and ductility [30].

2. Experimental

2.1. Materials

Linear low density polyethylene (LLDPE) was used as the polymer matrix material. LLDPE powder EL-lene M3804RWP was a commercial product purchased from SCG Chemicals Co., Ltd. It shows a melting point of 400 K and a melt flow index of 5 g/10 min (463 K/2.16 kg, ASTM D1238). The filler was a basalt fiber, roving RB-16-T5 (Tekhnobasalt LTD., Ukraine) of 16 μm in diameter. The fiber was processed in a staple apparatus of guillotine type. The cutting length was 1 ± 0.15 mm. The surface of the original basalt fiber was manufacturer-treated by solution of polydimethyl siloxane oligomer in ethanol as a surface wetting and lubricating agent.

2.2. Sample preparation

A polymer powder containing a fluidization agent (aerosol A300) is mixed with 10 wt% cut basalt fibers. The mixture is processed in a high-speed Henschel mixer in a stable turbulent mode under gradual increase in the filler content and the rotation speed

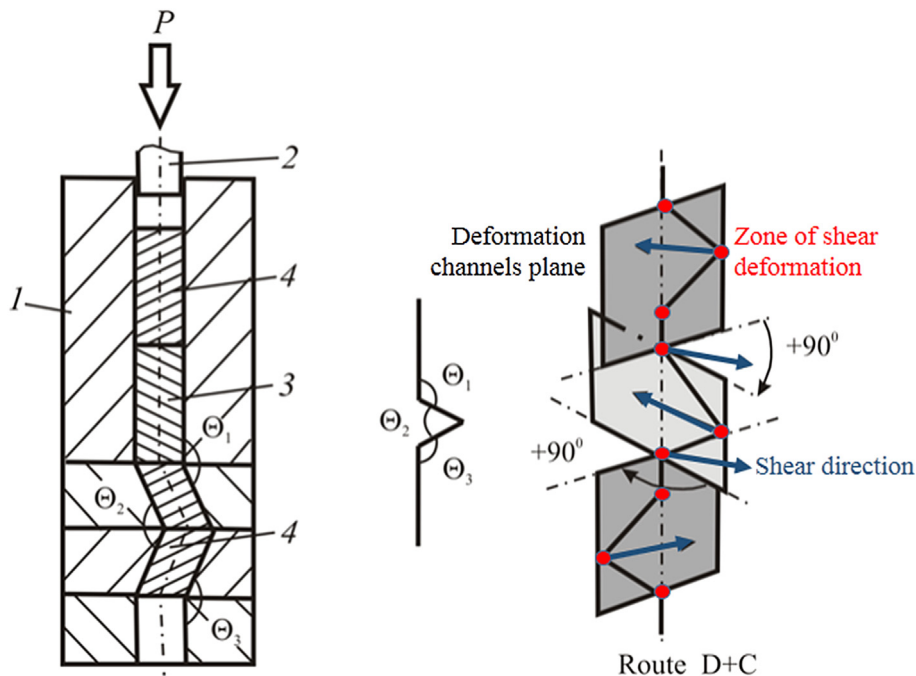


Fig. 1. Scheme of ECMAE process: 1- die, 2- punch, 3- polymeric billet, 4- sacrificed billets.

Table 1
Mechanical properties of the LLDPE and LLDPE/BFs composites.

Material	E , MPa	σ_y , MPa	ε_y , %	ΔH	α , kJ/m ²
LLDPE	190 ± 12	12.5 ± 1.4	34 ± 1	0.03	32 ± 2
LLDPE/BFs	228 ± 11	10.0 ± 1.2	21 ± 2	0.02	50 ± 2
Extruded LLDPE	291 ± 17	15.0 ± 1.5	35 ± 1	0.03	46 ± 2
Extruded LLDPE/BFs	370 ± 16	16.4 ± 1.2	42 ± 2	0.03	98 ± 3

of rotor ranging from 300 rpm (feeding) up to 1000–1200 rpm (mixing) in order to minimize bulling up of the filler. Due to fluidizing agent, powder composition is characterized by high flow rat. So, direct processing by a laboratory extruder with a rod-shaped end is possible, without the pelletization stage.

Processing of the composite mixture was carried out on the laboratory single screw extruder ($D = 25$ mm, $L/D = 25$) equipped with a rod-type die, at the screw speed of 25 rpm. The temperature profile along the heating zones was 413, 463, and 478 K from the feed section to the die, respectively.

The moulding tool in the form of a cylinder polished inside and a plunger was mounted at the die and heated up to 363 K. The forming was performed by fast filling of the cylinder from the extruder. The plunger was displaced by the ram pressure with the succeeding cooling of the moulding tool surface. In the course of cooling, the moulding tool was made up by the melt to compensate the shrinkage. The cooling time was 5–6 min. The obtained cylinder-shaped samples of 20 mm in diameter were machine processed to the required shape. Neat LLDPE was also processed under the same conditions to obtain a reference material.

As a method of solid-phase extrusion, ECMAE was selected. Fig. 1 demonstrates the ECMAE scheme. A polymer billet is pressed through a device consisting of several pairs of channels of the same diameter intersecting at varied angles Θ_i . The inlet and outlet channels are made vertically coaxial to keep the billet pointing to the right direction. The detailed description of ECMAE is presented in Ref. [37]. ECMAE was carried out at the deformation intensity $\Delta\Gamma = 0.83$, the accumulated strain $\varepsilon = 8.5$, the extrusion

temperature of 333 K and at the extrusion rate of 0.6 mm/s.

The control over the position of the shearing plane in the space guarantees different variants of deformation spatial development. Fig. 1 shows also the positions of deformation channels plane used in the work. As a deformation route, route D + C was selected. Here the pairs of oblique deforming channels are located in perpendicular planes rotated through the vertical axis in increments of 90°, and separated by vertical channels [37]. This configuration allows realization of simple shear in the planes perpendicular to the extrusion axis and in the planes arranged at an angle of $\pm 67.5^\circ$ to the extrusion axis. At the same time, the shear vector is rotated by an angle of 180° and depending on the deformation zone - by an angle of 90° (Fig. 1). The above processing condition allows for the generation of the maximal orientation of the LLDPE fibers parallel and normal to the extrudate's axis. Both the extrudates and the original billets were shaped as cylinders of 15 mm in diameter and 50 mm in length.

2.3. Mechanical and thermal properties

Tensile measurements were performed according to the ISO 527-2 standard. Specimens of the gauge length of 25 mm and the width of 5 mm (ISO 527-2, type 1BA) were cut out from the initial and extruded samples using a steel template. For extrudates specimens oriented along the extrusion directions were prepared. Specimens were tested at room temperature (295 K) using a universal testing machine Instron, Model 5582. The crosshead speed was constant and set to 1.25 mm/min, i.e. the initial deformation rate was 5%/min. The Young's modulus was determined from the stress-strain plots in the strain range up to 4%. Microindentation measurements were performed using a microhardness tester with a Vickers square-based diamond indenter (with the vertex angle of 136°). A detailed description of the measurement technique was reported in the paper [38]. The indenter was pressed into the sample at the loading of 0.5 N. The value of microhardness H was derived from the residual projected area of indentation according to the expression $H = KP/d^2$ (MPa), where P is the contact load

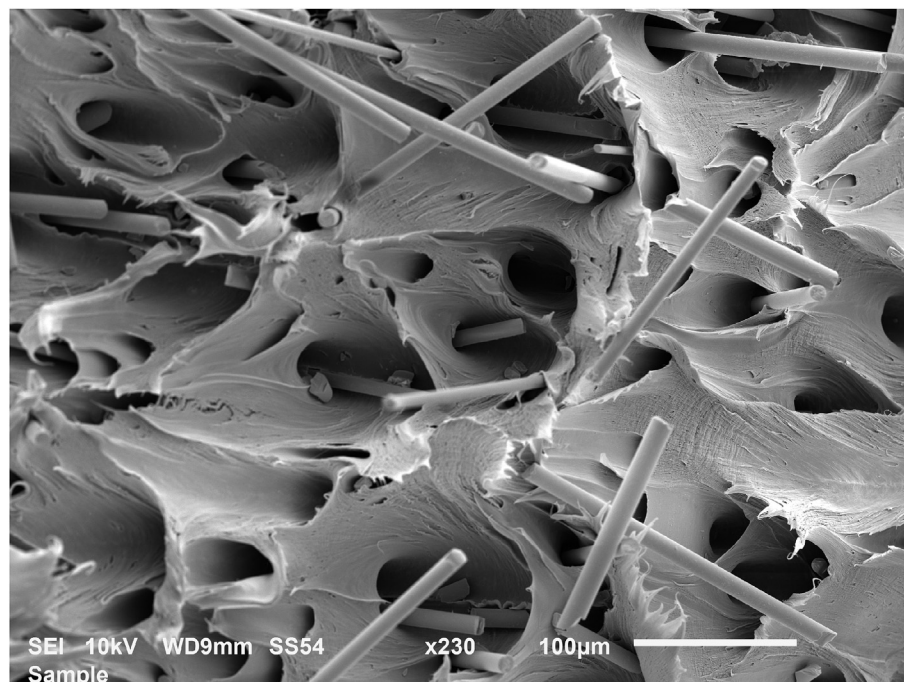


Fig. 2. SEM image of the fracture surface of the original LLDPE/BFs composite.

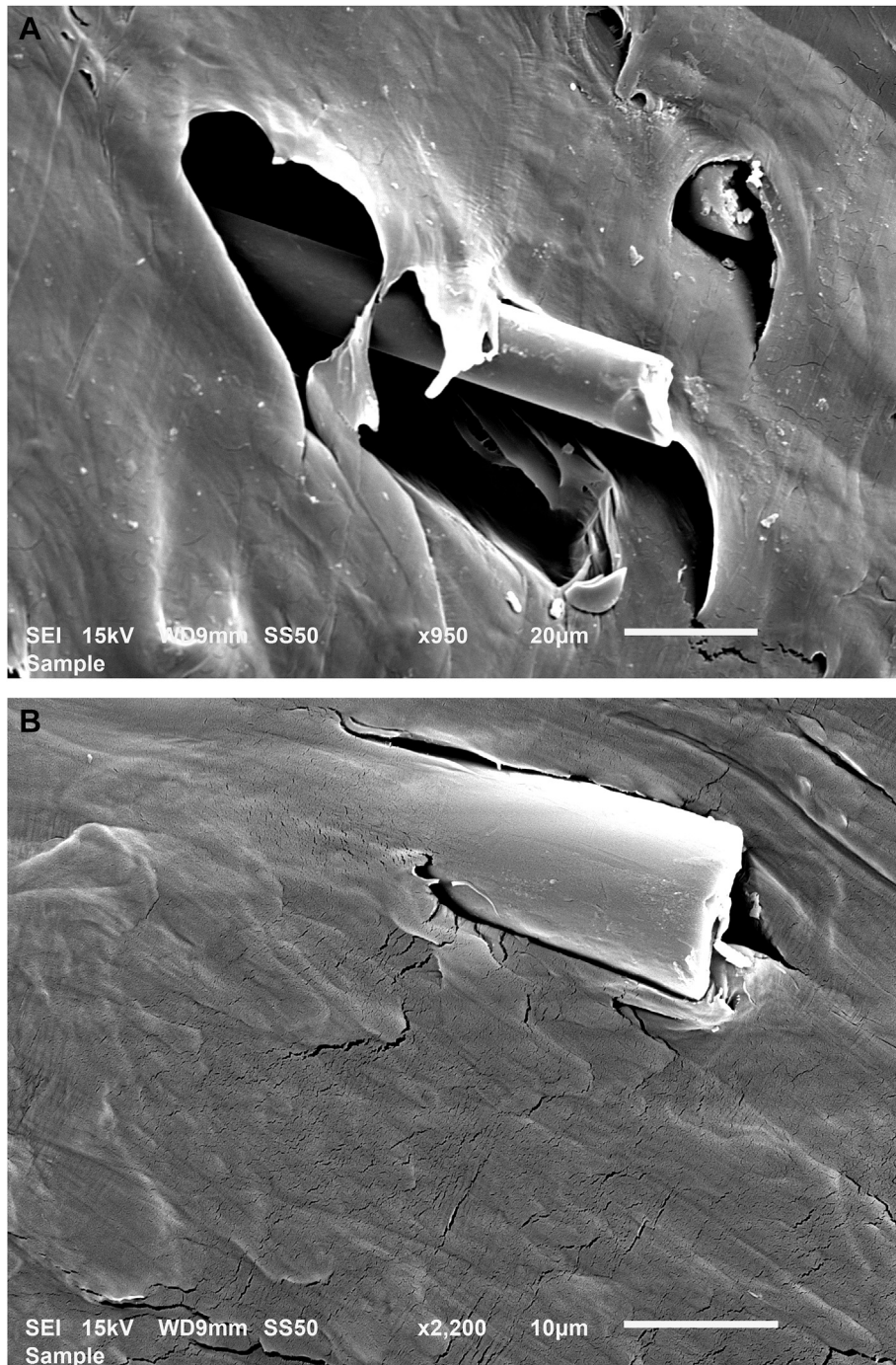


Fig. 3. SEM images of the fracture surface of the original LLDPE/BFs composite that illustrate weak (a) and strong (b) interface interaction between the polymer matrix and the basalt fiber.

applied in N ; d is the length of the impression diagonal in meters and k is a geometrical factor equal to 1.854 [38]. The length of the indenter diagonal was measured up to $1\ \mu\text{m}$ with an optical microscope. The value of microhardness anisotropy ΔH characterizing the difference in the strength properties in the longitudinal and transverse sections of extrudates is estimated by the formula [38]: $\Delta H = 1 - (\bar{H}^{\perp}/\bar{H}^{\parallel})$, where \bar{H}^{\perp} , \bar{H}^{\parallel} are the average values of microhardness in the transverse and longitudinal sections of extrudates, respectively. Notched Izod impact tests were carried out on a Ceast

6548/000 pendulum (energy: 4 J). The impact specimens used were 3.3 mm thick and their notches (depth = 2.54 mm and radius = 0.25 mm) were machined before and after ECMAE. A minimum of eight specimens was tested for each reported value in both the tensile and impact tests. Thermal behavior of samples was probed with DSC 2920 differential scanning calorimeter (TA Instruments) during heating from 300 K to 420 K with the rate of 10 K/min. Samples of the 7–8 mg mass were cut out from LLDPE and LLDPE/BFs composites and crimped in standard Al pans. The

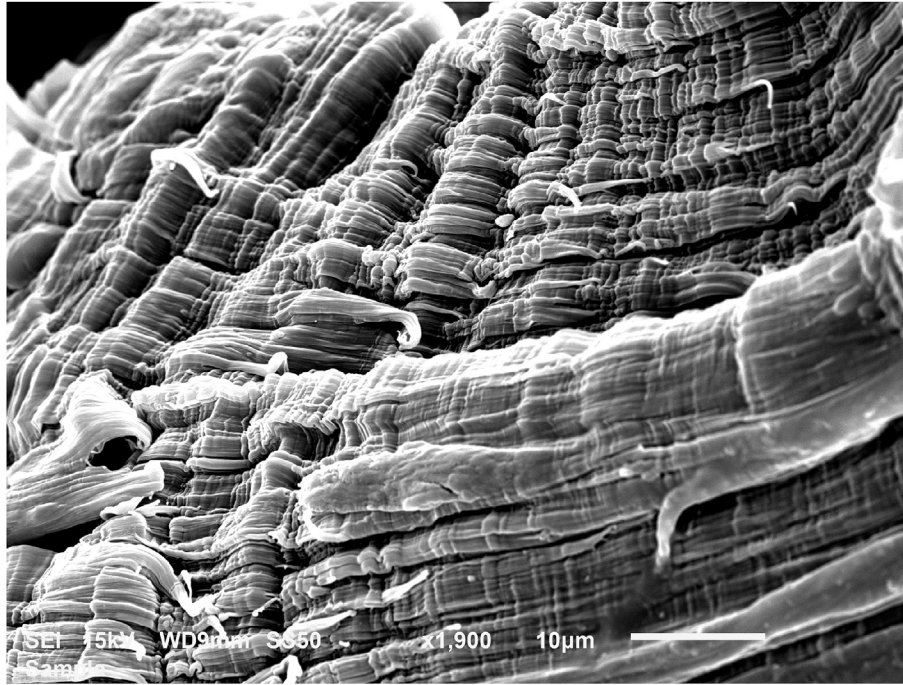


Fig. 4. SEM image of the fiber net in the extruded LLDPE.

DSC cell was purged with dry nitrogen during the measurements (20 ml/min). Enthalpy of fusion of 100% crystalline polyethylene was considered to be 293.6 J/g.

2.4. Scanning electronic microscopy

The composite morphology was analyzed by scanning electron microscopy (SEM) (JEOL JSM-5500 LV) after gold coating (Fine Coat Jeol Ion Sputter JEOL JFC-1200). The accelerating voltage was 15 kV. In order to determine the actual length of BFs, the LLDPE/BFs

composites were kept for 6 h in a muffle furnace at 723 K. The BFs samples taken from the muffle furnace were photographed for measurements of their length. The lengths of 600–800 fibers were measured for every sample studied.

2.5. Wide-angle X-ray scattering (WAXS)

WAXS investigation were done by using an X-ray diffractometer. Mn -filtrated FeK_{α} -radiation was used in this case. The patterns were taken in the diffraction mode (the Bragg-Bretano focusing). To

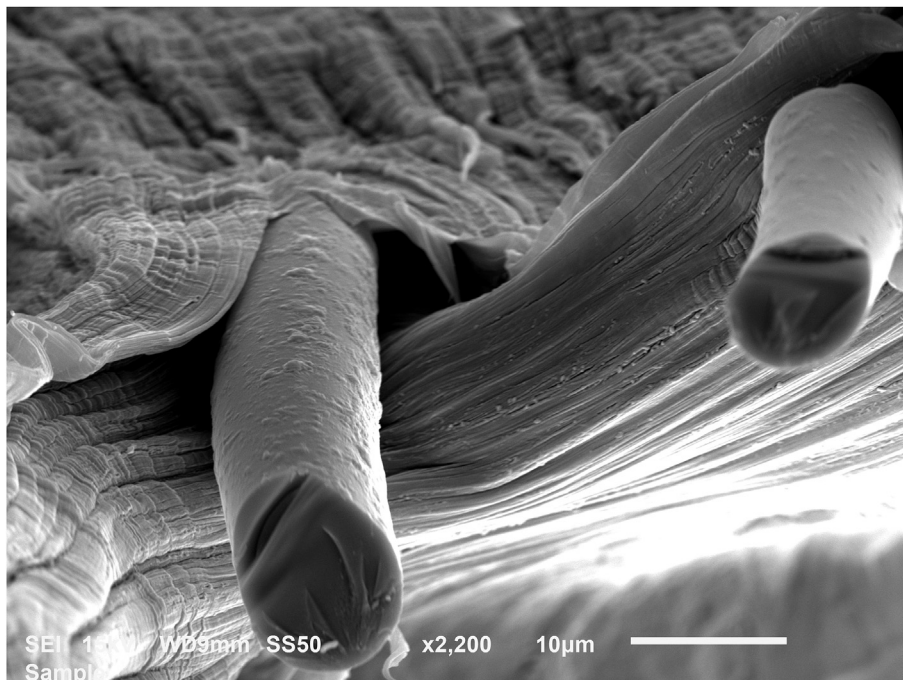


Fig. 5. SEM image of the contact area of the LLDPE fibers and the basalt fibers.

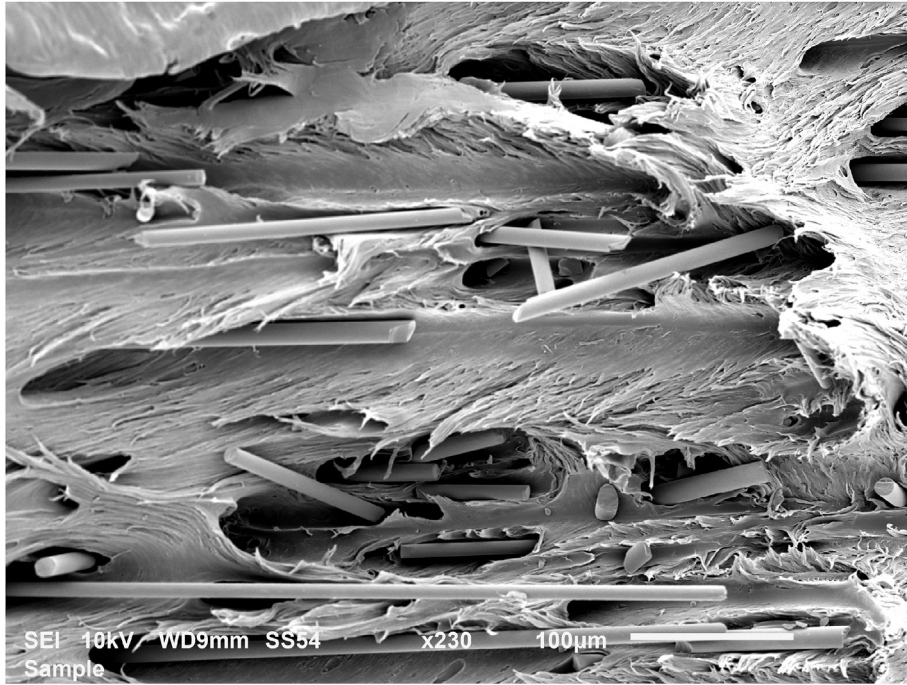


Fig. 6. SEM image of the fracture surface of the extruded LLDPE/BFs composite.

estimate the function of space orientation of crystallites, the scanning was accomplished in increments of 5° by the sample rotation in the azimuthal direction from the angle corresponding to the direction normal to the extrudate axis (these are angles of 90° and 270°). The detector was fixed at the scattering angle corresponding to the top of the diffraction maximum with the index of 200 with the top at 23.8°. As a measure of the total share of oriented material, the ratio of integral intensities of azimuthal scanning, I_{max} , within the angle range from 0° to 180° was used, being separated from

isotropic scattering to the total integral intensity.

3. Results and discussions

It is well known that strong fiber-reinforced effect can be obtained if the interfacial interaction between the polymer matrix and the filler fibers is strong enough. Strong interfacial interaction allows effective stress transfer from the polymeric matrix to rigid filler fibers. This process can be facilitated by formation of a net of

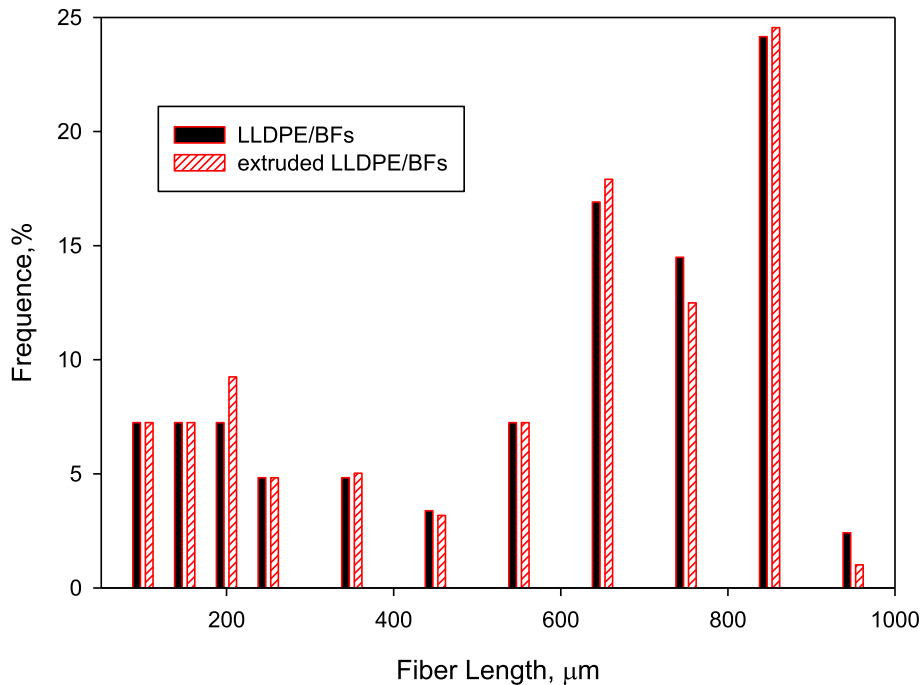


Fig. 7. Histograms of the BFs length distribution.

Biaxial LLDPE fiber stacking

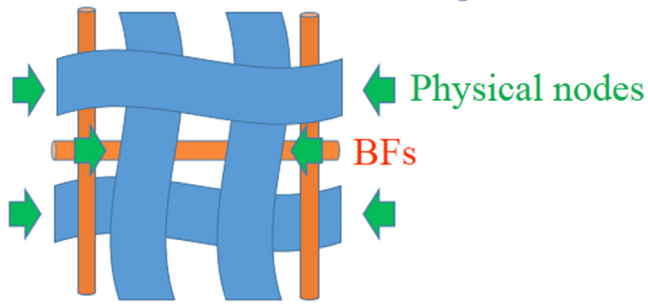


Fig. 8. Sketch of the LLDPE/BFs composite structure formed after ECMAE.

chemical and/or physical nodes between the polymer matrix and the filler fibers, and increased specific area of their contact. The mechanical data (average values) of LLDPE/BFs composites before and after solid-phase extrusion are collected in Table 1. It is seen that adding of BFs into the polymer matrix determines an increment in Young's modulus E and impact strength α . On the other hand, yield stress σ_y and yield strain ε_y are reduced. The behavior of σ_y and ε_y is typical of a number of polymeric systems [2,6,13]. It is associated with poor adhesion between the polar basalt fibers and the nonpolar LLDPE. The lack of interfacial bonds makes impossible efficient load transfer from the matrix to BFs. The presence of BFs results in continuity fault of the matrix and the related reduction of the maximum possible loading. An increase in E and α is associated with the presence of more rigid BFs and the fact that the filler fibers dissipate energy when they are pulled out of the matrix. The extrusion facilitates an increase in both α , E , and σ_y , ε_y . An increment of E and α in extruded LLDPE is lower than that of the extruded LLDPE/BFs composite. This fact indicates a contribution of BFs to the reinforcing effect.

Differences in tensile and impact properties of fiber filler based composites and fiber filler based self-reinforced ones can be

Table 2

Structural and thermal characteristics of the LLDPE and LLDPE/BFs composites.

Material	χ_c	T_{onset} , K	$T_{1\ max}$, K	$T_{2\ max}$, K
LLDPE	60.5	364.0	400.1	–
LLDPE/BFs	62.7	366.1	401.6	–
Extruded LLDPE	72.3	372.1	401.5	407.6
Extruded LLDPE/BFs	70.0	368.5	401.8	407.1

explained on the basis of the results of microstructure tests of the LLDPE/BFs composites before and after the solid-phase extrusion. A non-deformed composite is characterized by rather uniform distribution of BFs within the polymer matrix. The orientation of BFs is random (Fig. 2). At the same time, a number of fiber surfaces are not covered with the polymer (Fig. 3a); the traces of pulled out BFs are observed. This fact is indicative of poor adhesion between the LLDPE matrix and the BFs. At the same time, there exists a certain number of BFs characterized by a strong bond with the polymer matrix (Fig. 3b), that facilitate the reinforcement effect. ECMAE results in formation of a biaxial fibrillar structure in LLDPE (Fig. 4) that is similar to the structure of woven fabrics to some extent. In the case of extrusion of the LLDPE/BFs composite, an improvement of the interfacial interaction between the BFs and the LLDPE matrix takes place. This process is facilitated by the formation of a fibrillar structure in LLDPE accompanied by encapsulation of BFs by the LLDPE fibrils (Fig. 5). As a result, the frictional work is increased (more intensive energy dissipation occurs) in the course of the BFs pulling out as well as effective load transferring is provided.

The encapsulation is likely to be related to both formation of the LLDPE fibers and re-orientation of BFs in the course of ECMAE. The BFs are mostly arranged parallel and perpendicular to the longitudinal axis of the sample (Fig. 6). As compared to the random orientation, biaxial orientation of BFs is favorable with respect to the effectiveness of energy dissipation. The last phenomenon affects favorably the magnitude of the impact strength α of the fiber filler based self-reinforced composites. An important fact is that re-orientation does not affect the mean length of BFs (no mechanical

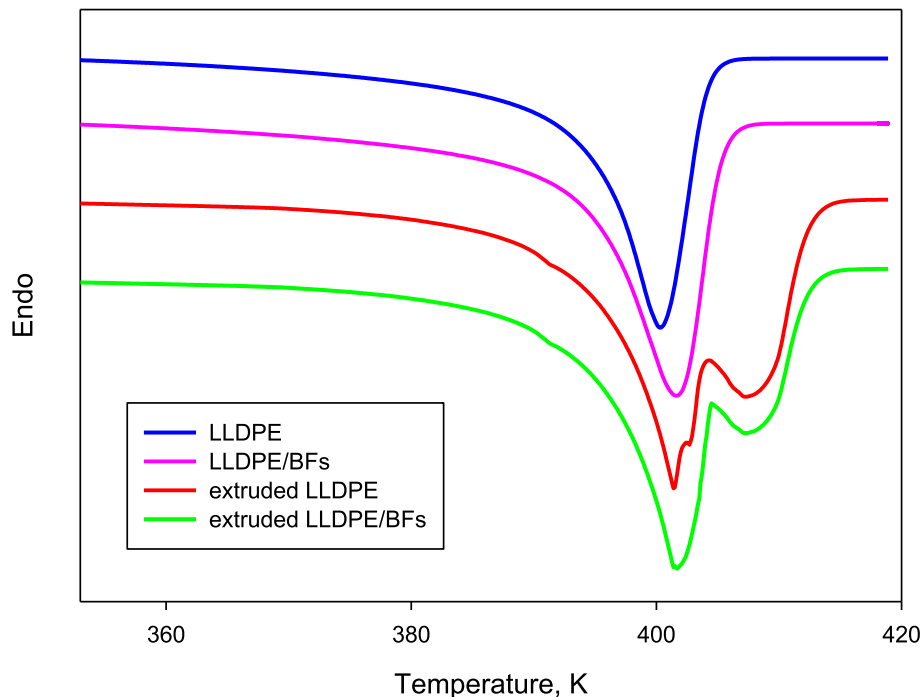


Fig. 9. DSC curves of the LLDPE and LLDPE/BFs composites.

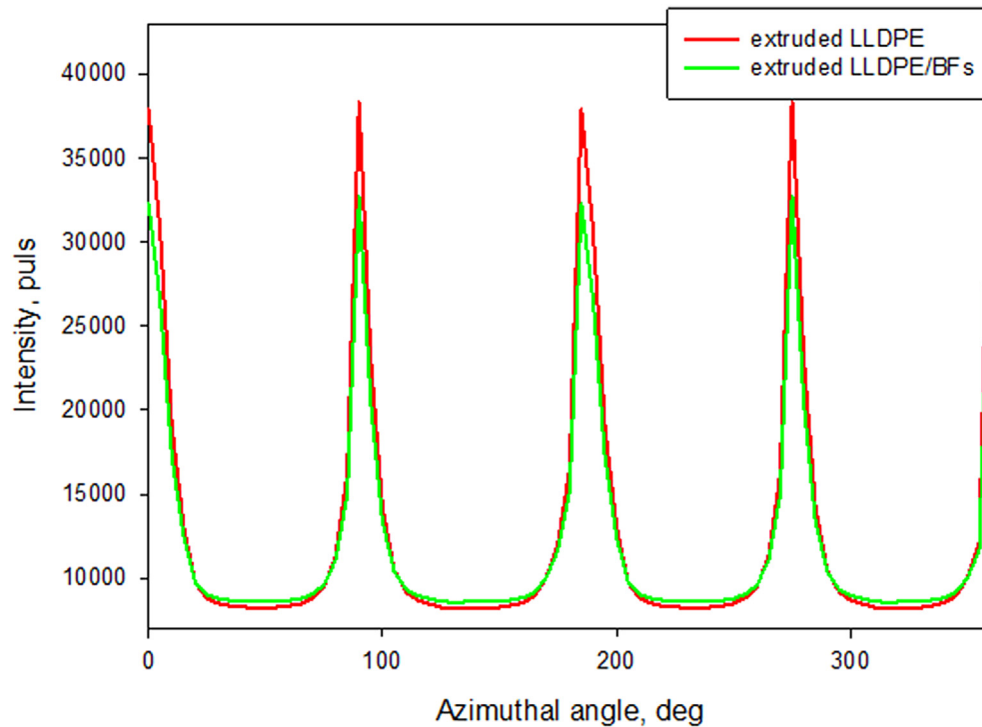


Fig. 10. Azimuth intensity profiles of the (200) LLDPE reflection.

destruction of the fibers occurs). The mean fiber length is about 760 μm that is close to the mean fiber length in non-extruded composites (770 μm). The character of the fiber lengths distribution is not almost modified, too (Fig. 7). It is known that the fiber lengths distribution and the fiber orientation distribution in fiber filler based composites are the key factors in determining the mechanical properties of composites [39]. As the magnitudes of the elastic and strength characteristics of composites are strongly dependent on the number of fibers aligned with the load direction, one can suggest that an increase in E and σ_y in the case of extruded LLDPE/BFs composite is related to a larger amount of the BFs oriented along the selected tension direction. Besides, as was reported in Refs. [39,40], the yield stress and Young's modulus of glass fiber reinforced composites in flow direction exceed those in the direction perpendicular to the flow direction. Thus, one can expect that the biaxial orientation of BFs is also more preferred as compared to the uniaxial orientation of BFs from the viewpoint of the degree of anisotropy of the elastic and strength characteristics of hybrid composites. Low anisotropy in the LLDPE/BFs composites is demonstrated by microhardness results (low value of microhardness anisotropy ΔH , Table 1). The scheme of the main structural features responsible for the registered hybrid effect in ECMAE-modified LLDPE/BFs composite is presented in Fig. 8. A net of interwoven LLDPE fibrils contributes to enhanced rigidity, strength and toughness; formation of an effective net of physical nodes between the LLDPE fibers and BFs supports their succeeding growth due to possible generation of an effective reinforcing structure.

Formation of the fibrillar structure in LLDPE is accompanied by an increase in the degree of crystallinity and formation of more perfect and larger crystals (Fig. 9, Table 2). It is seen that the onset temperature T_{onset} , the melting peak temperature T_{max} , the degree of crystallinity χ_{cl} of the self-reinforced LLDPE are increased. As mentioned in Refs. [41,42], an increment of the crystallinity degree can be related to the strain-induced crystallization. A rise of the onset temperature and the melting peak temperature as well as a

reduction of the half-width of the melting peak are associated with formation of larger and more perfect crystallites accompanied by a decrease in the dispersion of the crystallite thickness. However the main specific feature of the melting curve of LLDPE self-reinforced by ECMAE is the existence of double melting peaks that is connected with formation of two types of crystal structures characterized by different degree of perfection and thermal stability [42]. The low-temperature peak is close to the one of the non-extruded LLDPE and related to the crystals of non-deformed LLDPE matrix. However, the high-temperature peak is that of the oriented crystals in LLDPE fibers. Though the presence of the BFs weakens the strain-induced crystallization effect, it remains sufficiently strongly pronounced. As the right shoulder of the high-temperature melting peak of the extruded LLDPE is shifted towards higher temperatures as compared to the extruded LLDPE/BFs composite, one can suggest that the presence of BFs results in formation of more defective and less oriented fibrillar crystals of LLDPE. The DSC data correlate with the data of X-ray structure analysis (Fig. 10) positing that a total share of the fibrillar LLDPE crystals (i.e. preferred oriented in two direction: parallel and normal to the extrudate axis) is 52% and 46% in the case of self-reinforced LLDPE and BF-filled self-reinforced LLDPE, respectively.

4. Conclusions

The studies presented in the paper show that it is possible to fabricate a new type of fiber filler based hybrid composites in which a part of reinforcing fibers is formed directly out of the polymeric matrix in the course of solid-phase extrusion. The polymer fibers are well bonded to the polymer matrix. This fact sets them apart from foreign organic and inorganic fibers that are usually characterized by weak adhesion and the resulting weak reinforcing effect. Control of orientation of the polymeric fibers and the filler fibers (in particular, creation of biaxial orientation) allows formation of an effective net of physical entanglements and solution of the problem of poor adhesion between the filler fibers and the polymer matrix.

These fiber filler based hybrid composites are able to have many different engineering applications. Simplicity of fabrication, possible replacement of a part of ready-made foreign organic and inorganic fibers by the formed polymeric fibers can play a very important role in achieving a performance/cost balance.

References

- [1] Fukunaga H, Chou TW, Fukuda H. Strength of intermingled hybrid composites. *J Reinf Plast Compos* 1984;3(2):145–60.
- [2] Jawaid M, Abdul Khalil HPS. Cellulosic/synthetic fibre reinforced polymer hybrid composites: a review. *Carbohydr Polym* 2011;86:1–18.
- [3] Sathishkumar T, Naveen J, Satheshkumar S. Hybrid fiber reinforced polymer composites—a review. *J Reinf Plast Compos* 2014;33:454–71.
- [4] Gupta MK, Srivastava RK. Mechanical properties of hybrid fibers-reinforced polymer composite: a review. *Polym-Plast Techn Eng* 2016;55(6):626–42.
- [5] Gacitua W, Ballerini A, Zhang J. Polymer nanocomposites: synthetic and natural fillers a review. *Maderas Cienc Y Tecnol* 2005;7:159–78.
- [6] Dhand V, Mittal G, Rhee KY, Park SJ, Hui D. A short review on basalt fiber reinforced polymer composites. *Compos Part B – Eng* 2015;73:166–80.
- [7] Saba N, Tahir PM, Jawaid M. A review on potentiality of nano filler/natural fiber filled polymer hybrid composites. *Polymers* 2014;6:2247–73.
- [8] Jawahar P, Balasubramanian M. Influence of nanosize clay platelets on the mechanical properties of glass fiber reinforced polyester composites. *J Nanosci Nanotechnol* 2006;6:3973–6.
- [9] Kord B, Kiakojouri S. Effect of nanoclay dispersion on physical and mechanical properties of wood flour/polypropylene/glass fibre hybrid composites. *Bio-Resources* 2011;6:1741–51.
- [10] Lin GM, Xie GY, Sui GX, Yang R. Hybrid effect of nanoparticles with carbon fibers on the mechanical and wear properties of polymer composites. *Compos Part B – Eng* 2012;43(1):44–9.
- [11] Singh AP, Pal KR. Novel hybrid of clay, cellulose, and thermoplastics. I. Preparation and characterization of composites of ethylene–propylene copolymer. *J Appl Polym Sci* 2007;104:2672–82.
- [12] Fu SY, Xu G, Mai YW. On the elastic modulus of hybrid particle/short-fiber/polymer composites. *Compos Part B – Eng* 2002;33:291–9.
- [13] Botev M, Betchev H, Bikiaris D, Panayiotou C. Mechanical properties and viscoelastic behavior of basalt fiber-reinforced polypropylene. *J Appl Polym Sci* 1999;74:523–31.
- [14] Van De Velde K, Kiekens P. Thermoplastic pultrusion of natural fibre reinforced composites. *Compos Struct* 2001;54:355–60.
- [15] Kim MT, Kim MH, Rhee KY, Park SJ. Study on an oxygen plasma treatment of a basalt fiber and its effect on the interlaminar fracture property of basalt/epoxy woven composites. *Compos Part B – Eng* 2011;42(3):499–504.
- [16] Kurniawan D, Kim BS, Lee HY, Lim JY. Atmospheric pressure glow discharge plasma polymerization for surface treatment on sized basalt fiber/poly(lactic acid) composites. *Compos Part B – Eng* 2012;43(3):1010–4.
- [17] Wu Q, Chi K, Wu Y, Lee S. Mechanical, thermal expansion, and flammability properties of co-extruded wood polymer composites with basalt fiber reinforced shells. *Mater Des* 2014;60:334–42.
- [18] Dong C, Davies IJ. Flexural strength of bidirectional hybrid epoxy composites reinforced by E glass and T700S carbon fibres. *Compos Part B – Eng* 2015;72:65–71.
- [19] Ary Subagia IDG, Kim Y, Tijing LD, Kim CS, Shon HK. Effect of stacking sequence on the flexural properties of hybrid composites reinforced with carbon and basalt fibers. *Compos Part B – Eng* 2014;58:251–8.
- [20] Selmy AI, Elsesi AR, Azab NA, Abd El-baky MA. In-plane shear properties of unidirectional glass fiber (U)/random glass fiber (R)/epoxy hybrid and non-hybrid composites. *Compos Part B – Eng* 2012;43(2):431–8.
- [21] Valença SL, Griza S, Gomes de Oliveira V, Sussuchi EM, Carvalho de Cunha FG. Evaluation of the mechanical behavior of epoxy composite reinforced with Kevlar plain fabric and glass/Kevlar hybrid fabric. *Compos Part B – Eng* 2015;70:1–8.
- [22] Wu SH, Wang FY, Ma CCM, Chang WC. Mechanical, thermal and morphological properties of glass fiber and carbon fiber reinforced polyamide-6 and polyamide-6/clay nanocomposites. *Mater Lett* 2001;49:327–33.
- [23] Sandler JKW, Pegel S, Cadek M, Gojny F, van Es M, Lohmar J, et al. A comparative study of melt spun polyamide-12 fibres reinforced with carbon nanotubes and nanofibres. *Polymer* 2004;45:2001–15.
- [24] Park R, Jang J. Performance improvement of carbon fiber polyethylene fiber hybrid composites. *J Mater Sci* 1999;34(12):2903–10.
- [25] Sarasini F, Tirillò J, Ferrante L, Valente M, Valente T, Lampani L, et al. Drop weight impact behaviour of woven hybrid basalt–carbon/epoxy composites. *Compos Part B – Eng* 2014;59:204–20.
- [26] Zhang Y, Yu C, Chu PK, Lv F, Zhang C, Ji J, et al. Mechanical and thermal properties of basalt fiber reinforced poly(butylene succinate) composites. *Mater Chem Phys* 2012;133:845–9.
- [27] Hashmi SAR, Kitano T, Chand N. Dynamic mechanical behavior of LCP fiber/glass fiber-reinforced LLDPE composites. *Polym Compos* 2001;22(2):213–20.
- [28] García M, González N, Eguiazabal JI, Nazabal J. Structure and mechanical properties of new hybrid Composites based on polyamide 6,6 reinforced with both glass fibers and a semiaromatic liquid crystalline polyester. *Polym Compos* 2004;25(6):601–8.
- [29] Kmetty A, Bárány T, Karger-Kocsis J. Self-reinforced polymeric materials: a review. *Prog Polym Sci* 2010;35:1288–310.
- [30] Beloshenko VA, Voznyak YuV, Reshidova IYu, Naït-Abdelaziz M, Zairi F. Equal-channel angular extrusion of polymers. *J Polym Res* 2013;20:322.
- [31] Seo YR, Weon JI. Manipulation of nanofiller and polymer structures by using equal channel angular extrusion. *J Korean Physic Soc* 2013;63(1):114–9.
- [32] Li H, Huang X, Huang C, Zhao Y. An investigation about solid equal channel angular extrusion on polypropylene/organic montmorillonite composite. *J Appl Polym Sci* 2012;123:2222–7.
- [33] Weon JI, Sue HJ. Effects of clay orientation and aspect ratio on mechanical behavior of Nylon-6 nanocomposite. *Polymer* 2005;46:6325–34.
- [34] Weon JI, Xia ZY, Sue HJ. Morphological characterization of Nylon-6 nanocomposite following a large-scale simple shear process. *J Polym Sci Part B Polym Phys* 2005;43:3555–66.
- [35] Ma J, Simon GP, Edward GH. The effect of shear deformation on Nylon-6 and two types of Nylon-6/clay nanocomposite. *Macromolecules* 2008;41:409–20.
- [36] Creasy TS, Kang YS. Fibre fracture during equal-channel angular extrusion of short fibre-reinforced thermoplastics. *J Mater Proc Tech* 2005;160:90–8.
- [37] Beloshenko VA, Voznyak AV, Voznyak YuV. Control of the mechanical and thermal properties of semicrystalline polymers via a new processing route of the equal channel multiple angular extrusion. *Polym Eng Sci* 2014;54:531–9.
- [38] Baltá Calleja FJ. Microhardness relating to crystalline polymers. *Adv Polym Sci* 1985;66:117–48.
- [39] Ary Subagia IDG, Kim Y, Tijing LD, Kim CS, Shon HK. Effect of stacking sequence on the flexural properties of hybrid composites reinforced with carbon and basalt fibers. *Compos Part B – Eng* 2014;58:251–8.
- [40] Mortazavian S, Fatemi A. Effect of fiber orientation and anisotropy on tensile strength and elastic modulus of short fiber reinforced polymer composites. *Compos Part B – Eng* 2015;72:116–29.
- [41] Galeski A. Strength and toughness of crystalline polymer systems. *Prog Polym Sci* 2003;28(12):1643–99.
- [42] Beloshenko VA, Voznyak YuV, Mikhal'chuk VM. A microcalorimetric study of crystallizable polymers subjected to severe plastic deformation. *Polym Sci Ser A – Polym Phys* 2014;56:269–74.